JOURNAL OF THERMOPHYSICS AND HEAT TRANSFER
Vol. 9, No. 3, July–September 1995

# Scattering Characteristics of Fibrous Media Containing Closely Spaced Parallel Fibers

Siu-Chun Lee* and Jan A. Grzesik†
*Applied Sciences Laboratory, Inc., Hacienda Heights, California 91745*

**The theoretical formulation for scattering by a semi-infinite medium containing closely spaced, parallel fibers at oblique incidence is presented in this article. The fibers can be either coated or uncoated, and their diameters are comparable to the wavelength of the incident radiation and spacing between the fibers. The radiative propagation characteristics, which include the propagation constant and amplitude of the effective wave in the medium, are derived by a rigorous solution of Maxwell's relations by accounting for the multiple dependent scattering effects. Formulas are also developed for the coherent and incoherent scattered intensities. Numerical results are presented to illustrate the scattering behavior of dense fibrous media containing alumina-coated silica fibers and Rayleigh limit silica fibers.**

## Nomenclature

$a^{\sigma}_{jn}$ = dependent scattering wave coefficient, transverse electric mode
${}^{0}a^{\sigma}_{jn}$ = independent scattering wave coefficient, transverse electric mode
$b^{\sigma}_{jn}$ = dependent scattering wave coefficient, transverse magnetic mode
${}^{0}b^{\sigma}_{jn}$ = independent scattering wave coefficient, transverse magnetic mode
$C_e$ = extinction cross section
$C_s$ = scattering cross section
$\boldsymbol{E}$ = electric field
$\boldsymbol{e}$ = unit vector
$f_v$ = volume fraction of fibers, $\pi r_0^2 n_0 L_0$
$G^{jn}_{ks}$ = function defined by Eq. (3)
$g(R)$ = radial distribution function
$\boldsymbol{H}$ = magnetic field
$H_n$ = Hankel function of the second kind
$h$ = $k_0 \sin \phi_i$
$\boldsymbol{I}^{\sigma}_{c}$ = coherent scattering intensity function
$\boldsymbol{I}^{\sigma}_{ic}$ = incoherent scattering intensity distribution
$i$ = $\sqrt{-1}$
$J_n$ = Bessel function
$\boldsymbol{K}^{\sigma}$ = effective propagation constant of the fibrous medium, $K^{\sigma}\boldsymbol{e}_t$
$K^{\sigma}$ = magnitude of $\boldsymbol{K}^{\sigma}$
$k$ = imaginary part of complex refractive index $m$, or index from 1 to $N_0$
$k_0$ = propagation constant of medium containing the fibers
$L$ = $K^{\sigma} \cos \phi_t$
$L_0$ = average fiber length
$l_0$ = $k_0 \cos \phi_i$
$m$ = complex refractive index of fiber, $n - ik$
$N_0$ = total number of fibers
$n$ = real part of complex refractive index, or index, $-\infty$ to $\infty$
$n_0$ = number of fibers per unit volume
$\boldsymbol{n}_r$ = unit vector in the coherent scattered direction
$Q_e$ = extinction efficiency
$R$ = magnitude of $\boldsymbol{R}$
$\boldsymbol{R}$ = radial vector
$R_{jk}$ = radial distance between the centers of fibers $j$ and $k$
$r_0$ = radius of fiber
$s$ = index, $-\infty$ to $\infty$
$t$ = time
$u$ = scalar potential function, transverse magnetic mode
$V$ = volume of medium
$v$ = scalar potential function, transverse electric mode
$W_0$ = width of medium under observation along $Y$ axis
$X^{\sigma}_n$ = transverse magnetic mode amplitude of the effective wave
$Y^{\sigma}_n$ = transverse electric mode amplitude of the effective wave
$\alpha$ = size parameter, $2\pi r_0/\lambda$
$\gamma$ = polar angle measured from the $X$ axis
$\gamma_{jk}$ = angle that the line joining the centers of fibers $j$ and $k$ makes with the $X$ axis
$\delta$ = phase angle, Eq. (47)
$\delta_{jk}$ = Kronecker delta function
$\varepsilon_j$ = phase shift of the primary incident wave at fiber $j$ relative to the origin
$\theta$ = azimuthal angle of incident or transmitted wave
$\lambda$ = wavelength
$\tau$ = $+1$ for transverse magnetic mode, $-1$ for transverse electric mode
$\phi$ = polar angle of the incident or transmitted wave
$\omega$ = circular frequency

*Subscripts*

$i$ = incident wave
$j, k$ = index, refers to the fiber
$n, s$ = index, $-\infty$ to $\infty$
$r$ = radial direction
$t$ = transmitted wave
$x$ = $x$ direction
$y$ = $y$ direction
$z$ = $z$ direction

*Superscripts*

$I$ = transverse magnetic mode
$II$ = transverse electric mode
$s$ = scattering
$\sigma$ = mode of the incident radiation, $I$ or $II$
$*$ = complex conjugate

Presented as Paper 94-2904 at the AIAA/ASME 6th Joint Thermophysics and Heat Transfer Conference, Colorado Springs, CO, June 20–23, 1994; received July 5, 1994; revision received Dec. 12, 1994; accepted for publication Dec. 16, 1994. 

*Vice President, Senior Member AIAA.
†Senior Scientist.

## Introduction

DEVELOPMENT of advanced thermal insulation materials that can withstand very high temperatures and heat fluxes is generally recognized as a critical technology issue for many future aerospace and energy systems. Many thermal protection materials such as building insulations and Space Shuttle tile materials are high-porosity fibrous media containing randomly oriented fibers. Thermal-structural materials such as the refractory liners and many fiber-reinforced composites are high-density media that contain closely spaced, aligned fibers. Radiative energy transfer through a dispersed medium containing fibers or spheres is strongly influenced by the size, index of refraction, and in particular, the concentration of the scatterers.

In a high-porosity fibrous medium, independent scattering prevails because the separation between fibers is much greater than the fiber diameter and the wavelength of the incident radiation. Each fiber acts as an isolated scatterer, and the radiative transfer equation, which assumes independent scattering, is applied. In a high-density fibrous medium, near-field multiple scattering becomes dominant because the fiber-spacing is comparable to the fiber diameter and wavelength.[1,2] Neglecting near-field multiple scattering in a finite configuration of closely spaced parallel fibers has been shown to yield nonphysical results.[3] A rigorous theoretical treatment that accounts for dependent scattering is, therefore, essential to the accurate analysis of the scattering characteristics of high-density fibrous media.

Earlier analyses on scattering by closely spaced fibers considered only normal incidence on a finite configuration of homogeneous fibers.[4-6] The general multiple scattering formalisms for oblique incidence on homogeneous and radially stratified fibers were developed by Lee.[7,8] Formulas for the extinction, absorption, and scattering cross sections, as well as the scattering intensity distribution function, were derived for arbitrary fiber diameter, spatial location, and wavelength. In principle, these formulations can be applied to analyze high-density fibrous media by specifying the location and properties of all the fibers. This approach becomes impractical when the number of fibers is large, e.g., exceeding about 100, due to the excessive demand on computer assets.

Radiative propagation through dense fibrous media is usually analyzed by a statistical approach that assumes a random distribution of fibers of identical properties. This approach involves the averaging of the multiple-scattering wave equations for a random distribution of fibers. Lax's quasicrystalline approximation (QCA)[9] is then applied to solve for the propagation constant of the average wave. This method has been applied to develop the dispersion relation for the effective propagation constants of dense fibrous media at normal incidence.[10-13] The general dispersion relations for oblique incidence on fibrous media containing homogeneous or coated fibers were developed by Lee.[14,15] These formulations are applicable to arbitrary fiber size, refractive index, concentration, and wavelength, as well as a dielectric matrix medium. For a dielectric medium with nonunity refractive index, the wavelength and fiber refractive index relative to the medium would be used, i.e., the implicit parameter shift of scaling the refractive index of the fiber and the freespace wavelength by the refractive index of the medium is applied in the dispersion relations.

The complete characterization of the radiative behavior of high-density fibrous media requires both the effective propagation constant and scattering amplitude. While the former is given by the dispersion relation, the scattering amplitude still needs to be solved. The objective of this article is to present the formulations for the scattering amplitude and scattering characteristics of semi-infinite fibrous media containing closely spaced, coated or uncoated, parallel fibers. The semi-infinite medium assumption is usually satisfied by high-density fibrous media because of their large extinction coefficient and optical depth due to the high solid volume fraction.

## Theory

The theoretical formulation for the scattering characteristics of high-density fibrous media is developed by a rigorous solution of Maxwell's equations. In the following sections, the scattering characteristics of a finite configuration of closely spaced, parallel fibers are first summarized. A new, more compact equation for the scattering cross section is presented. The theoretical treatment for a semi-infinite high-density fibrous medium then follows. This includes the formulations for the scattering amplitude and the coherent and incoherent scattered intensities. Finally, numerical results on the scattering behavior of fibrous media containing alumina-coated silica fibers and Rayleigh limit silica fibers are presented for the purpose of illustration.

### Scattering Characteristics of a Finite Configuration of Fibers

Figure 1 depicts a medium containing closely spaced, parallel, homogeneous or radially stratified fibers. The fibers are parallel to the $Z$ axis and are located to the right of the origin. The incident radiation propagates in an arbitrary oblique direction defined by the unit vector $\boldsymbol{e}_i = \cos\phi_i \cos\theta_i \boldsymbol{e}_x - \cos\phi_i \sin\theta_i \boldsymbol{e}_y + \sin\phi_i \boldsymbol{e}_z$, where $\phi_i$ and $\theta_i$ are the polar and azimuthal angles, respectively, and $\boldsymbol{e}_x$, $\boldsymbol{e}_y$, and $\boldsymbol{e}_z$ are unit vectors along the coordinate axes. The propagation constant of the medium containing the fibers is $k_0$. The wave coefficients $b^{\sigma}_{jn}$ and $a^{\sigma}_{jn}$ that account for multiple scattering are related to the scattering properties and location of the fibers by[7,8]

$$\sum_{s=-\infty}^{\infty} \sum_{k=1}^{N_0} \left[ \{\delta_{jk}\delta_{ns} + (1-\delta_{jk}) G^{jn}_{ks}\,{}^0b^{I}_{jn}\} b^{\sigma}_{jn} + \{(1-\delta_{jk}) G^{jn}_{ks}\,{}^0b^{II}_{jn}\} a^{\sigma}_{jn} \right] = \varepsilon_j\,{}^0b^{\sigma}_{jn} \exp(in\theta_i) \tag{1}$$

$$\sum_{s=-\infty}^{\infty} \sum_{k=1}^{N_0} \left[ \{(1-\delta_{jk}) G^{jn}_{ks}\,{}^0a^{I}_{jn}\} b^{\sigma}_{jn} + \{\delta_{jk}\delta_{ns} + (1-\delta_{jk}) G^{jn}_{ks}\,{}^0a^{II}_{jn}\} a^{\sigma}_{jn} \right] = \varepsilon_j\,{}^0a^{\sigma}_{jn} \exp(in\theta_i) \tag{2}$$

where

$$G^{jn}_{ks} = (-i)^{s-n} H_{s-n}(l_0 R_{jk}) \exp[i(s-n)\gamma_{kj}] \tag{3}$$

${}^0b^{\sigma}_{jn}$ and ${}^0a^{\sigma}_{jn}$ are the wave coefficients for an isolated fiber, $\varepsilon_j = \exp(-i\boldsymbol{k}\cdot\boldsymbol{R}_j)$ is the phase shift of the incident wave at fiber $j$, $\boldsymbol{k} = k_0\boldsymbol{e}_i$, and the subscript $\sigma = I, II$ refers to the mode of the incident wave. Specifically, $\sigma = I$ refers to the transverse magnetic (TM) mode, and $\sigma = II$ refers to the transverse electric (TE) mode. The formulas for the wave coefficients of isolated homogeneous and coated fibers are summarized in Refs. 16 and 17, respectively.

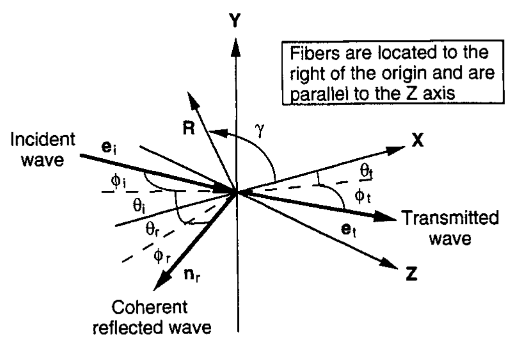


**Fig. 1 Schematic diagram showing an electromagnetic wave at oblique incidence on a fibrous medium.**

Utilizing the optical extinction theorem, the extinction cross section of the fiber configuration per unit length of fiber is given by[7,8]

$$C_e^\sigma = \frac{2\lambda}{\pi} \operatorname{Re} \sum_{j=1}^{N_0} \sum_{n=-\infty}^{\infty} \exp\{il_0 R_{kj} \cos(\gamma_{kj} + \theta_i)\}\{b_{jn}^\sigma + a_{jn}^\sigma\} \tag{4}$$

where Re denotes taking the real part, and the center of fiber $k$ is arbitrarily chosen as the reference origin. The scattering cross section is obtained by integrating the scattering intensity distribution. A more compact expression than that reported previously is obtained as

$$C_s^\sigma = \frac{2\lambda}{\pi} \sum_{j=1}^{N_0} \sum_{k\neq j}^{N_0} \sum_{n=-\infty}^{\infty} \sum_{s=-\infty}^{\infty} \exp\{i(n - s)(\gamma_{kj} - \pi/2)\} \times J_{s-n}(l_0 R_{kj})\{b_{jn}^\sigma b_{ks}^{\sigma*} + a_{jn}^\sigma a_{ks}^{\sigma*}\} \tag{5}$$

where the superscript * denotes the complex conjugate.

**Scattering Characteristics of Dense Fibrous Media**

In a high-density fibrous medium the separation between fibers is comparable to the wavelength of the incident radiation and the diameter of the fibers. To obtain the radiative characteristics of a dense fibrous medium, the conditional averages of Eqs. (1) and (2) are taken, which yield a system of equations involving successively higher order averages. The hierarchy of multiple scattering terms is truncated by applying the QCA, which states that[9]

$$\{\langle a_{jn}^\sigma\rangle_{jk}, \langle b_{jn}^\sigma\rangle_{jk}\} = \{\langle a_{jn}^\sigma\rangle_j, \langle b_{jn}^\sigma\rangle_j\} \tag{6}$$

where the angle brackets $\langle\ \rangle$ denote conditional averaging, and the subscripts $j$ and $k$ outside the bracket indicate that the average is performed by holding the fibers corresponding to the subscripts fixed. The waves inside the medium are assumed to propagate with an effective propagation constant $\boldsymbol{K}^\sigma$ as

$$\{\langle b_{jn}^\sigma\rangle_j, \langle a_{jn}^\sigma\rangle_j\} = \{X_n^\sigma, Y_n^\sigma\}\exp(-i\boldsymbol{K}^\sigma \cdot \boldsymbol{R}_j) \tag{7}$$

where $X_n^\sigma$ and $Y_n^\sigma$ are the amplitudes of the average wave, $\boldsymbol{K}^\sigma = K^\sigma \boldsymbol{e}_t$, $\boldsymbol{e}_t = \cos\phi_t \cos\theta_t \boldsymbol{e}_x - \cos\phi_t \sin\theta_t \boldsymbol{e}_y + \sin\phi_t \boldsymbol{e}_z$ is the unit vector in the propagating direction of the effective wave, and $\phi_t$ and $\theta_t$ are complex polar and azimuthal angles, respectively. The directions of the incident and transmitted waves are related by Snell's law as

$$k_0 \cos\phi_i \sin\theta_i = K^\sigma \cos\phi_t \sin\theta_t \tag{8}$$

$$k_0 \sin\phi_i = K^\sigma \sin\phi_t \tag{9}$$

where $\phi_t$ and $\theta_t$ are different for the TM and TE mode waves. Taking the conditional averages of Eqs. (1) and (2) yields

$$X_n^\sigma = \varepsilon_j {}^0b_n^\sigma \exp(i\boldsymbol{K}^\sigma \cdot \boldsymbol{R}_j + in\theta_i) - \sum_{s=-\infty}^{\infty} ({}^0b_n^I X_s^\sigma + {}^0b_n^{II} Y_s^\sigma) F_{sn} \tag{10}$$

$$Y_n^\sigma = \varepsilon_j {}^0a_n^\sigma \exp(i\boldsymbol{K}^\sigma \cdot \boldsymbol{R}_j + in\theta_i) - \sum_{s=-\infty}^{\infty} ({}^0a_n^I X_s^\sigma + {}^0a_n^{II} Y_s^\sigma) F_{sn} \tag{11}$$

where $F_{sn} = F_{sn,1} + F_{sn,2} + F_{sn,3}$. It should be pointed out that the cross-mode terms $Y_n^I$ and $X_n^{II}$ vanish at normal incidence. The evaluation of $F_{sn,1}$, $F_{sn,2}$, and $F_{sn,3}$ involves transformations utilizing the Helmholtz equations for the propagation constants $K^\sigma$ and $k_0$, respectively, Green's second identify, and Gauss's theorem. $F_{sn,1}$ is the integral over the volume containing a pair of nonpenetrating fibers, which is given by[15]

$$F_{sn,1} = \frac{2f_v}{r_0^2} \frac{\exp\{i(n - s)\theta_i\}}{k_0^2 - K^{\sigma 2}} \{2l_0 r_0 J_{s-n}(2Lr_0) H'_{s-n}(2l_0 r_0) - 2Lr_0 H_{s-n}(2l_0 r_0) J'_{s-n}(2Lr_0)\} \tag{12}$$

where $f_v = \pi r_0^2 n_0 L_0$ is the fiber volume fraction, $n_0$ is the number of fibers per unit volume, $L_0$ is the average fiber length, $L = K^\sigma \cos\phi_t$, and the superscript $'$ denotes differentiation with respect to the argument. $F_{sn,2}$ involves the radial distribution $g(R)$ of fibers as[15]

$$F_{sn,2} = \frac{2f_v}{r_0^2} \exp\{i(n-s)\theta_i\} \times \int_{2r_0}^{\infty} J_{s-n}(LR) H_{s-n}(l_0 R)\{g(R) - 1\} R \, \mathrm{d}R \tag{13}$$

The function $F_{sn,3}$ involves the evaluation over the entire volume of the semi-infinite fibrous medium $V_0$:

$$F_{sn,3} = \int_{V_0} \exp[i\boldsymbol{K}^\sigma \cdot (\boldsymbol{R}_j - \boldsymbol{R}_k)] G_{ks}^{jn} \, \mathrm{d}V_k = \frac{f_v}{\pi r_0^2} \frac{\exp(iK_x^\sigma x_j)}{K^{\sigma 2} - k_0^2} \times \left(iK_x^\sigma - \frac{\partial}{\partial x_{kj}}\right) \int_{-\infty}^{\infty} \exp(-iK_y^\sigma y_{kj}) G_{ks}^{jn} \, \mathrm{d}y_{jk}\big|_{x_k=0} \tag{14}$$

where $k_x = l_0 \cos\theta_i$ and $K_x^\sigma = L \cos\theta_t$. The evaluation of Eq. (14) involves first the expansion of $G_{ks}^{jn}$ in the far field, then the transformation of the integrand into cylindrical polar coordinates, and finally the evaluation by the method of stationary phase. After extensive manipulations, we obtain

$$F_{sn,3} = -i\beta^\sigma \exp\{i(n-s)\theta_i\}\exp\{i(K_x^\sigma - k_x)x_j\} \tag{15}$$

where

$$\beta^\sigma = \frac{2f_v}{\pi r_0^2} \frac{1}{k_x(K_x^\sigma - k_x)} \tag{16}$$

Substituting Eqs. (12–15) into Eqs. (10) and (11) results in two expressions, each containing two groups of terms with different propagation constants. One group is associated with $K^\sigma$ for the propagation of the effective wave within the medium, which gives the Lorentz–Lorentz law

$$\sum_{s=-\infty}^{\infty} \{[\delta_{ns} + {}^0b_n^I(F_{sn,1} + F_{sn,2})]X_s^\sigma + {}^0b_n^{II}(F_{sn,1} + F_{sn,2})Y_s^\sigma\} = 0 \tag{17}$$

$$\sum_{s=-\infty}^{\infty} \{{}^0a_n^I(F_{sn,1} + F_{sn,2})X_s^\sigma + [\delta_{ns} + {}^0a_n^{II}(F_{sn,1} + F_{sn,2})]Y_s^\sigma\} = 0 \tag{18}$$

In order for a nontrivial solution of the amplitudes to exist, the determinant of the above system of homogeneous equations must vanish. Equating the determinant to zero gives the dispersion equation that governs the effective propagation constant $K^\sigma$.[14,15] The other group of terms is associated with $k_0$, which balances the incident wave with the reflected wave at the interface boundary. This group yields two equations given by

$$\sum_{s=-\infty}^{\infty} \exp(-is\theta_i)\{X_s^\sigma, Y_s^\sigma\} = (i/\beta^\sigma)\{\delta_{\sigma I}, \delta_{\sigma II}\} \tag{19}$$

where $\delta_{\sigma I}$ and $\delta_{\sigma II}$ are Kronecker delta functions.

The scattering amplitudes $X_s^\sigma$ and $Y_s^\sigma$ are determined by utilizing Eq. (19) in conjunction with the homogeneous systems of equations given by Eqs. (17) and (18). It can be shown that the amplitudes of the dominant modes are an even function of the Fourier index $n$:

$$\{X_n^I, Y_n^{II}\} = \{X_{-n}^I, Y_{-n}^{II}\} \tag{20}$$

whereas, the amplitudes of the cross-mode terms are an odd function of $n$:

$$\{X_n^{II}, Y_n^I\} = \{-X_{-n}^{II}, -Y_{-n}^I\} \tag{21}$$

In addition, the zeroth-order term of the cross-mode amplitudes vanishes as

$$X_0^{II} = Y_0^I = 0 \tag{22}$$

The effective propagation constant and scattering amplitudes of the effective wave yield all the information for predicting radiative transfer through the fibrous medium. In the following sections the formulations for the coherent and incoherent scattering behavior of semi-infinite high-density fibrous media are presented.

**Coherent Scattering Characteristics**

The time-averaged Poynting vector for the coherent scattered intensity is defined as

$$\boldsymbol{S}_c^\sigma = \tfrac{1}{2}\,\mathrm{Re}\{\langle \boldsymbol{E}^{\sigma s}\rangle \times \langle \boldsymbol{H}^{\sigma s}\rangle^*\} \tag{23}$$

where $\langle \boldsymbol{E}^{\sigma s}\rangle$ is the conditional average of the scattered electric field including contributions from all the fibers, $\langle \boldsymbol{H}^{\sigma s}\rangle^* = i\nabla \times \langle E^{\sigma s}\rangle^*/(\omega\mu_0)$ is the complex conjugate of the magnetic field, $\omega$ is the angular frequency, and $\mu_0$ is the permeability constant of the medium. The total scattered electric field from all the fibers is given by

$$\langle \boldsymbol{E}^{\sigma s}\rangle = \left\langle \sum_{j=1}^{N_0} \boldsymbol{E}_j^{\sigma s}\right\rangle = n_0\left\{-\nabla \times \left(\boldsymbol{e}_z F_0 \int_{V_0} \langle v_j^{\sigma s}\rangle\, \mathrm{d}V_j\right) + \frac{i}{k_0}\nabla \times \nabla \times \left(\boldsymbol{e}_z F_0 \int_{V_0} \langle u_j^{\sigma s}\rangle\, \mathrm{d}V_j\right)\right\} \tag{24}$$

where $F_0 = \exp(i\omega t - ihz)$, $h = k_0 \sin\phi_i$

$$u_j^{\sigma s}(R_{jp}) = -\tau F_0 \sum_{n=-\infty}^{\infty} (-i)^n \exp(in\gamma_{jp}) b_{jn}^\sigma H_n(l_0 R_{jp}) \tag{25}$$

$$v_j^{\sigma s}(R_{jp}) = \tau F_0 \sum_{n=-\infty}^{\infty} (-i)^n \exp(in\gamma_{jp}) a_{jn}^\sigma H_n(l_0 R_{jp}) \tag{26}$$

are the $z$ components of the Hertz potentials for fiber $j$, $\tau = 1$ for $\sigma = I$, and $\tau = -1$ for $\sigma = II$. Equation (24) can be readily evaluated in the far-field asymptotic limit to give the coherent scattered intensity function $\boldsymbol{I}_c^\sigma = \boldsymbol{S}_c^\sigma/S_0$ as

$$\boldsymbol{I}_c^\sigma = |\beta^\sigma \rho^\sigma|^2\{|I_c^{\sigma-I}|^2 + |I_c^{\sigma-II}|^2\}\boldsymbol{n}_r \tag{27}$$

where $S_0 = l_0^2/\{2\sqrt{\mu_0/\varepsilon_0}\}$ is the incident flux, $\varepsilon_0$ is the permittivity constant of the medium

$$\rho^\sigma = (K_x^\sigma - k_x)/(K_x^\sigma + k_x) \tag{28}$$

is the reflection coefficient

$$I_c^{\sigma-I} = \sum_{n=-\infty}^{\infty} (-1)^n X_n^\sigma \exp(in\theta_i) \tag{29}$$

$$I_c^{\sigma-II} = \sum_{n=-\infty}^{\infty} (-1)^n Y_n^\sigma \exp(in\theta_i) \tag{30}$$

are the components of the coherent scattered radiation, and

$$\boldsymbol{n}_r = -\cos\phi_i \cos\theta_i \boldsymbol{e}_x - \cos\phi_i \sin\theta_i \boldsymbol{e}_y + \sin\phi_i \boldsymbol{e}_z \tag{31}$$

is the unit vector in the specular direction. It is evident from $\boldsymbol{e}_i$ and $\boldsymbol{n}_r$ that the angles of incidence and reflection are equal as dictated by Snell's law. By utilizing Eqs. (20–22), the coherent scattering components are given by

$$I_c^{I-I} = X_0^I + 2\sum_{n=1}^{\infty} (-1)^n X_n^I \cos(n\theta_i) \tag{32}$$

$$I_c^{I-II} = 2i\sum_{n=1}^{\infty} (-1)^n Y_n^I \sin(n\theta_i) \tag{33}$$

for a TM mode incident wave, and

$$I_c^{II-I} = 2i\sum_{n=1}^{\infty} (-1)^n X_n^{II} \sin(n\theta_i) \tag{34}$$

$$I_c^{II-II} = Y_0^{II} + 2\sum_{n=1}^{\infty} (-1)^n Y_n^{II} \cos(n\theta_i) \tag{35}$$

for a TE mode incident wave.

**Incoherent Scattering Characteristics**

The incoherent scattered radiation is equal to the difference between the total and the coherent scattered radiation. The time-averaged incoherent Poynting vector is

$$\begin{aligned}\boldsymbol{S}_{ic}^\sigma &= \tfrac{1}{2}\,\mathrm{Re}\langle(\boldsymbol{E}^{\sigma s} - \langle \boldsymbol{E}^{\sigma s}\rangle) \times (\boldsymbol{H}^{\sigma s} - \langle \boldsymbol{H}^{\sigma s}\rangle)^*\rangle \\ &= \tfrac{1}{2}\,\mathrm{Re}\{\langle \boldsymbol{E}^{\sigma s} \times \boldsymbol{H}^{\sigma s^*}\rangle - \langle \boldsymbol{E}^{\sigma s}\rangle \times \langle \boldsymbol{H}^{\sigma s}\rangle^*\}\end{aligned} \tag{36}$$

where the first term is the total scattered radiation and the second term is the coherent scattered radiation. By using the asymptotic expansion of the Hankel function in Eqs. (25) and (26), the scattered electric field for fiber $j$ in the far field becomes

$$\boldsymbol{E}_j^{\sigma s} = \tau i l_0 F_0 \sum_{n=-\infty}^{\infty} \left[a_{jn}^\sigma \boldsymbol{e}_r \times \boldsymbol{e}_z + \frac{b_{jn}^\sigma}{k_0}(h\boldsymbol{e}_r - l_0\boldsymbol{e}_z)\right] \times \sqrt{\frac{2i}{\pi l_0 R_p}} \exp[in\gamma_{jp} - il_0(R_p - \boldsymbol{R}_j \cdot \bar{\boldsymbol{R}}_p)] \tag{37}$$

where $\boldsymbol{e}_r$ is the unit radial vector in the $XY$ plane, $\bar{\boldsymbol{R}}_p$ is the unit vector along $\boldsymbol{R}_p$, and the far-field approximation $R_{jp} \approx R_p$ is made. The far-field scattered magnetic field for fiber $j$ is obtained by taking the curl of the electric field, which yields

$$\boldsymbol{H}_j^{\sigma s} = (1/\omega\mu_0)(l_0\boldsymbol{e}_r + h\boldsymbol{e}_z) \times \boldsymbol{E}_j^{\sigma s} \tag{38}$$

By utilizing Eqs. (37) and (38), the total scattered radiation can be obtained as

$$\langle \boldsymbol{E}^{\sigma s} \times \boldsymbol{H}^{\sigma s^*}\rangle = \left\langle \sum_{j=1}^{N_0} \boldsymbol{E}_k^{\sigma s} \times \sum_{k=1}^{N_0} \boldsymbol{H}_k^{\sigma s^*}\right\rangle = \boldsymbol{e}_s \frac{2l_0}{\pi R_p}\frac{k_0}{\omega\mu_0} \times \left\langle \sum_{j=1}^{N_0}\sum_{k=1}^{N_0}\sum_{n=-\infty}^{\infty}\sum_{m=-\infty}^{\infty} \exp[i(n-m)\gamma]\{a_{jn}^\sigma a_{km}^{\sigma^*} + b_{jn}^\sigma b_{km}^{\sigma^*}\}\{\delta_{jk} + (1-\delta_{jk})\exp[-il_0(\boldsymbol{R}_k - \boldsymbol{R}_j)\cdot \bar{\boldsymbol{R}}_p]\}\right\rangle \tag{39}$$

where $\gamma \sim \gamma_{ip}$ in the far field and $e_s = \cos\phi_i e_r + \sin\phi_i e_z$ is the unit vector along the incoherent scattered direction. Examination of $e_s$ indicates that the incoherent scattered radiation propagates along the surface of a cone with an apex angle $\pi - 2\phi_i$ as in the case of an isolated infinite cylinder.

The conditional average of the diagonal terms, i.e., $j = k$, in Eq. (39) can be readily evaluated as

$$\left\langle \sum_{j=1}^{N_0} (a_{jm}^{\sigma} a_{jm}^{\sigma*} + b_{jm}^{\sigma} b_{jm}^{\sigma*}) \right\rangle \approx n_0 \int_{V_0} \{\langle a_{jm}^{\sigma}\rangle_j \langle a_{jm}^{\sigma*}\rangle_j + \langle b_{jm}^{\sigma}\rangle_j \langle b_{jm}^{\sigma*}\rangle_j\} \,\mathrm{d}V_j \tag{40}$$

To evaluate the off-diagonal terms, i.e., $j \neq k$, the distorted Born approximation is applied. This yields

$$\left\langle \sum_{j=1}^{N_0} \sum_{k\neq j}^{N_0} a_{jm}^{\sigma} a_{km}^{\sigma*} \exp[-il_0(\boldsymbol{R}_k - \boldsymbol{R}_j)\cdot \bar{\boldsymbol{R}}_p] \right\rangle \approx n_0^2 \int_{V_0}\int_{V_0} \langle a_{jm}^{\sigma}\rangle_j \langle a_{km}^{\sigma*}\rangle_k \exp[-il_0(\boldsymbol{R}_k - \boldsymbol{R}_j)\bar{\boldsymbol{R}}_p] \times g(R_{jk}) \,\mathrm{d}V_j \,\mathrm{d}V_{jk} \tag{41}$$

which represents a first-order approximation to account for the near-field interactions between the fibers. The conditional average of the term involving $b_{jm}^{\sigma} b_{km}^{\sigma*}$ can be written similarly.

By utilizing Eqs. (24) and (39–41) in Eq. (36), and subtracting the coherent scattering term from the total scattered radiation, the incoherent scattered intensity distribution function is obtained as

$$\begin{aligned} \boldsymbol{I}_{ic}^{\sigma}(\gamma) &= \frac{S_{ic}^{\sigma} R_p}{S_0 W_0 \cos\phi_i \cos\theta_i} \\ &= \boldsymbol{e}_s \frac{f_v}{\pi^2\alpha^2} (\cos^2\phi_i \cos\theta_i K_{ix}^{\sigma}/k_0)^{-1} \\ &\times \{1 + \mathrm{Re}\,\Psi^{\sigma}(\gamma)\}\{|I_{ic}^{\sigma-I}(\gamma)|^2 + |I_{ic}^{\sigma-II}(\gamma)|^2\} \end{aligned} \tag{42}$$

where

$$I_{ic}^{\sigma-I}(\gamma) = \sum_{n=-\infty}^{\infty} X_n^{\sigma} \exp(in\gamma) \tag{43}$$

$$I_{ic}^{\sigma-II}(\gamma) = \sum_{n=-\infty}^{\infty} Y_n^{\sigma} \exp(in\gamma) \tag{44}$$

In the above expressions, $K_{ix}^{\sigma} = -\mathrm{Im}\,K_x^{\sigma}$, Im denotes the imaginary part, $W_0$ is the width of the strip along the $Y$ axis under observation, and $\pi/2 \leq \gamma \leq 3\pi/2$ is the range of the backscattering angle. The function $\Psi^{\sigma}$ is given by

$$\Psi^{\sigma}(\gamma) = n_0 L_0 \int_{S_0\to\infty} \exp(i\,\mathrm{Re}\,\boldsymbol{K}^{\sigma}\cdot\boldsymbol{R}_{jk} - il_0\boldsymbol{R}_{jk}\cdot\bar{\boldsymbol{R}}_p) \times [g(R_{jk}) - 1]\,\mathrm{d}S_{jk} = \frac{2f_v}{r_0^2}\left\{\psi_0^{\sigma} + 2\sum_{n=1}^{\infty}\psi_n^{\sigma}\cos n(\gamma+\delta)\right\} \tag{45}$$

where $S_0$ is the surface enclosing a pair of nonpenetrating fibers, and

$$\psi_n^{\sigma} = \int_{2r_0}^{\infty} J_n(\zeta R) J_n(l_0 R)[g(R) - 1] R \,\mathrm{d}R \tag{46}$$

$$\delta = \tan^{-1}(k_0 \cos\phi_i \sin\theta_i/\mathrm{Re}\,K_x^{\sigma}) \tag{47}$$

$$\zeta = \sqrt{(\mathrm{Re}\,K_x^{\sigma})^2 + (k_0\cos\phi_i \sin\theta_i)^2} \tag{48}$$

By utilizing Eqs. (20–22), we can write

$$I_{ic}^{I-I}(\gamma) = X_0^I + 2\sum_{n=1}^{\infty} X_n^I \cos(n\gamma) \tag{49}$$

$$I_{ic}^{I-II}(\gamma) = 2i\sum_{n=1}^{\infty} Y_n^I \sin(n\gamma) \tag{50}$$

for a TM mode incident wave, and

$$I_{ic}^{II-I}(\gamma) = 2i\sum_{n=1}^{\infty} X_n^{II} \sin(n\gamma) \tag{51}$$

$$I_{ic}^{II-II}(\gamma) = Y_0^{II} + 2\sum_{n=1}^{\infty} Y_n^{II} \cos(n\gamma) \tag{52}$$

for a TE mode incident wave.

### Rayleigh Limit Approximation

For completeness, expressions for the coherent and incoherent scattered intensities in the Rayleigh limit, i.e., $\alpha \ll 1$, are also presented. In the Rayleigh limit only amplitudes of order $n = -1, 0, 1$ remain dominant. In addition, only the zeroth-order term in Eq. (45) remains, and $\Psi^{\sigma}$ then becomes a constant independent of the mode of the incident wave:

$$\Psi_R = 8f_v \int_1^{\infty} [g(R) - 1]R\,\mathrm{d}R \tag{53}$$

where the subscript $R$ denotes the Rayleigh limit. Based on statistical theorems, Twersky[18] showed that a closed-form approximation of Eq. (53) can be obtained as

$$\Psi_R = \frac{(1 - f_v)^3}{(1 + f_v)^3} - 1 \tag{54}$$

The coherent scattered intensity function follows from Eqs. (27), (32), and (33) as

$$I_c^I = |\beta^{\sigma}\rho^{\sigma}|^2\{|X_0^I - 2X_1^I\cos\theta_i|^2 + |2Y_1^I \sin\theta_i|^2\}\boldsymbol{n}_r \tag{55}$$

$$I_c^{II} = |\beta^{\sigma}\rho^{\sigma}|^2\{|Y_0^{II} - 2Y_1^{II}\cos\theta_i|^2 + |2X_1^{II}\sin\theta_i|^2\}\boldsymbol{n}_r \tag{56}$$

The incoherent scattered intensity distributions follow from Eqs. (42) and (53) as

$$\boldsymbol{I}_{ic}^{I}(\gamma) = \boldsymbol{e}_s \frac{f_v}{\pi^2\alpha^2}(\cos^2\phi_i\cos\theta_i K_{ix}^{\sigma}/k_0)^{-1}\frac{(1-f_v)^3}{(1+f_v)^3} \times \{|X_0^I + 2X_1^I\cos\gamma|^2 + |2Y_1^I\sin\gamma|^2\} \tag{57}$$

$$\boldsymbol{I}_{ic}^{II}(\gamma) = \boldsymbol{e}_s \frac{f_v}{\pi^2\alpha^2}(\cos^2\phi_i\cos\theta_i K_{ix}^{\sigma}/k_0)^{-1}\frac{(1-f_v)^3}{(1+f_v)^3} \times \{|Y_0^{II} + 2Y_1^{II}\cos\gamma|^2 + |2X_1^{II}\sin\gamma|^2\} \tag{58}$$

## Results

Numerical results are presented to illustrate the coherent and incoherent scattering characteristics of high-density fibrous media containing alumina-coated silica fibers and Rayleigh limit silica fibers. For the coated fibers the silica core is 1 $\mu$m in diameter, and the alumina coating is 0.5 $\mu$m thick, thus giving an o.d. of 2 $\mu$m. For the purpose of illustration, incident radiation at $\lambda = 2$ and 10 $\mu$m are considered. The optical properties of silica are $m = 1.438 - 4.7\mathrm{E}{-}06i$ at $\lambda = 2$ $\mu$m and $m = 2.62 - 0.28i$ at $\lambda = 10$ $\mu$m. For alumina $m = 1.737$ at $\lambda = 2$ $\mu$m and $m = 0.87 - 0.027i$ at $\lambda = 10$ $\mu$m. The fiber volume fraction is assumed to be 0.5. The incident

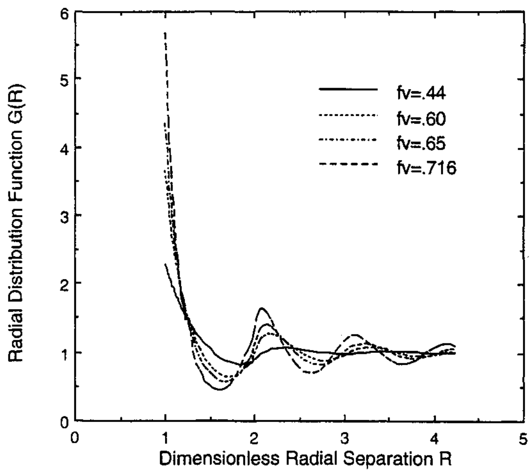


Fig. 2 Radial distribution functions of an $NpT$ ensemble of a hard disk fluid by Wood.[19]

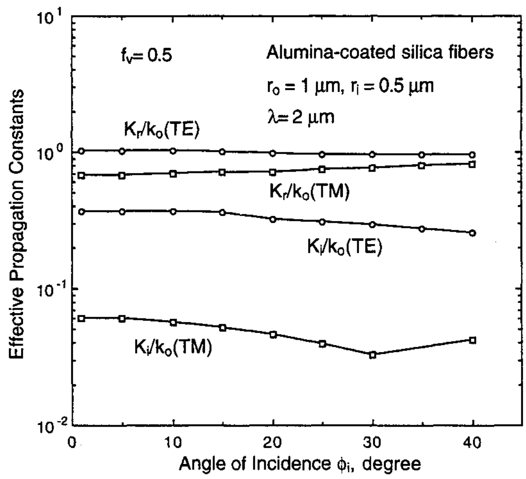


Fig. 3 Effective propagation constant of a medium of alumina-coated silica fibers at $\lambda = 2\ \mu m$.

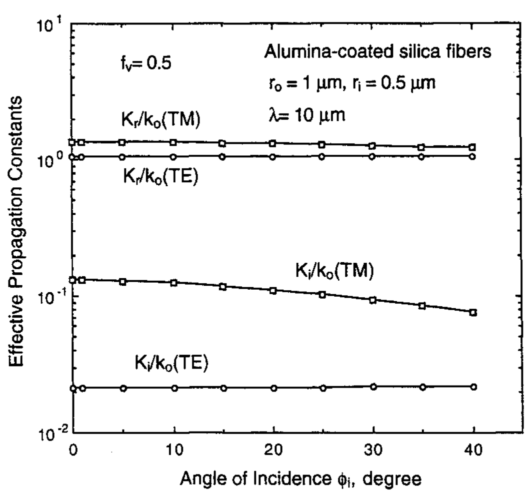


Fig. 4 Effective propagation constant of a medium of alumina-coated silica fibers at $\lambda = 10\ \mu m$.

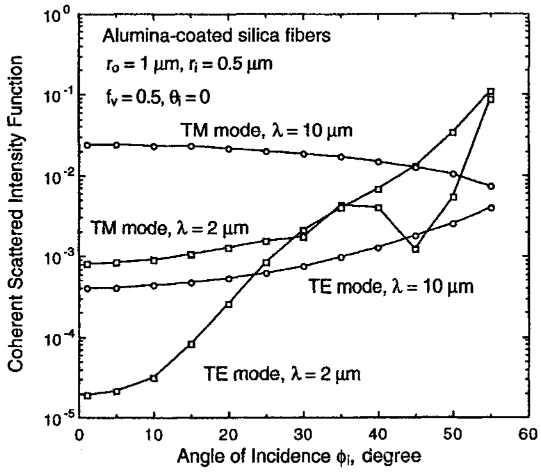


Fig. 5 Variation of the coherent scattered intensity function with incident angle.

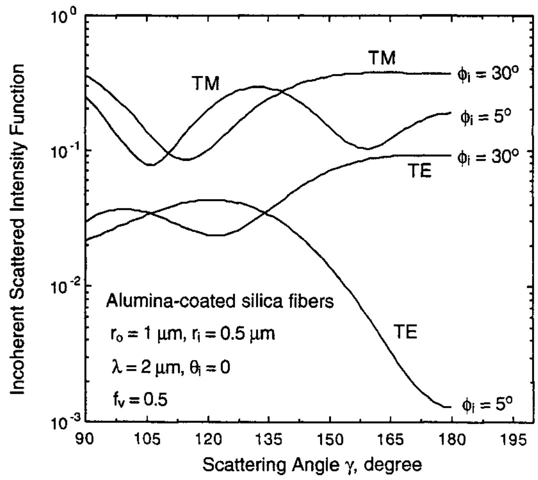


Fig. 6 Incoherent scattering intensity distribution function at $\lambda = 2\ \mu m$.

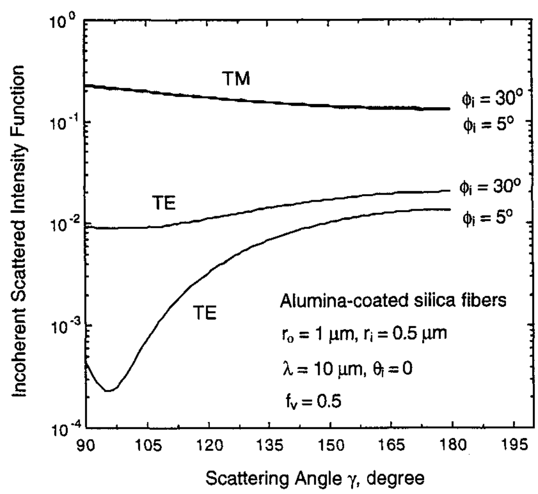


Fig. 7 Incoherent scattering intensity distribution function at $\lambda = 10\ \mu m$.

direction is assumed to be in the $XZ$ plane, i.e., $\theta_i = 0$. The radial distribution function $g(R)$ has been obtained by Wood[19] based on Monte Carlo analyses of isothermal–isobaric hard disk ensembles. Figure 2 shows several $g(R)$ for different solid volume fractions. For the purpose of illustration, the $g(R)$ approximating a volume fraction of 0.44 is used in the present numerical analyses for both the fibrous media containing alumina-coated silica fibers and Rayleigh limit silica fibers.

The variations of the complex effective propagation constants with incident angle at $\lambda = 2$ and $10\ \mu m$ are shown in Figs. 3 and 4, respectively. The real part $K_r/k_0$ generally deviates slightly from unity, whereas, the imaginary part is much smaller. It should be pointed out that the effective propagation constant $K^o$ is independent of the azimuthal angle of incidence $\theta_i$. The effective propagation constant is complex due to absorption and scattering. The real part is a measure

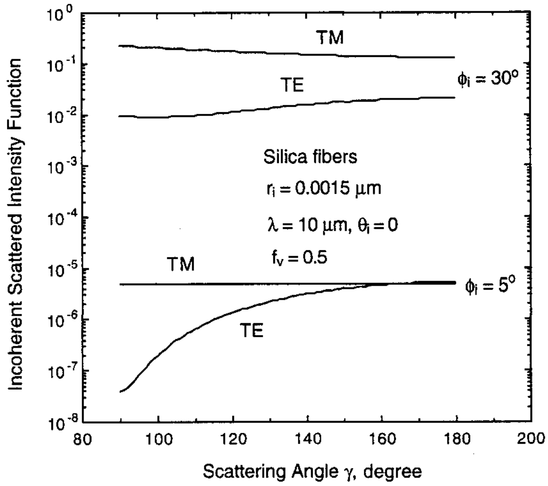


**Fig. 8 Incoherent scattering intensity distribution function for Rayleigh limit fibers at $\lambda = 10\ \mu m$.**

of the phase velocity of radiative propagation in the fibrous medium, and the imaginary part is related to the extinction efficiency of the medium by $Q_e = \pi\alpha K_i/(f_v k_0)$. A complex propagation constant also indicates that the surfaces of constant phase and constant amplitude do not coincide, which has been discussed in Ref. 15. Figure 5 shows the variation of the coherent scattered intensity [Eq. (27)] with incident angle, which is the radiation scattered in the specular direction. Figures 6 and 7 show the incoherent scattered intensity distribution at $\lambda = 2$ and $10\ \mu m$, respectively, for two incident angles. The incoherent scattered intensity distributions are shown for the TM and TE modes separately in order to illustrate their respective characteristics. They display more pronounced angular variation at $\lambda = 2\ \mu m$ than at $\lambda = 10\ \mu m$, due to the different size parameters ($\alpha = 3.14$ at $\lambda = 2\ \mu m$; $\alpha = 0.628$ at $\lambda = 10\ \mu m$) and optical properties. At $\lambda = 2\ \mu m$, the fibers are purely scattering, whereas the fibers are strongly absorbing at $\lambda = 10\ \mu m$.

For completeness, the incoherent scattered intensity distributions for Rayleigh limit silica fibers are shown in Fig. 8. The incident wavelength is assumed to be $10\ \mu m$, and the fiber radius is $0.0015\ \mu m$, giving a size parameter of 0.00094. As shown in the figure, the TM mode intensity is almost independent of the scattering angle, because the zeroth-order TM–TM mode scattering amplitude ($X_0^i$) dominates. For a TE mode incident wave, all of the scattering amplitudes are comparable, thus giving a more pronounced angular variation.

## Summary

High-density fibrous materials are widely used for thermal insulation in high-temperature applications. In particular, many fiber-reinforced composites used in thermal–structural applications contain unidirectional, closely spaced fibers. Because heat transfer by conduction and radiation is comparable at elevated temperatures, an accurate radiative analysis is needed to characterize the thermal performance and thermal–structural characteristics of a fibrous composite. Due to the small spacing between the fibers, dependent scattering is important, which must be accounted for in the evaluation of the thermal radiative properties of high-density fibrous media.

This article presented the theoretical formalism for the radiative properties of semi-infinite media containing closely spaced, parallel-coated or uncoated fibers at oblique incidence. The radiative propagation characteristics, which are the propagation constant and amplitude of the effective wave, are formulated by a rigorous consideration of Maxwell's theory. The coherent and incoherent scattering properties are formulated by accounting for the dependent scattering interactions in the medium. The present theoretical formalisms are applicable to arbitrary fiber size, optical properties, and wavelength. Numerical results are also presented to illustrate the scattering characteristics of semi-infinite media containing a 50% concentration of alumina-coated silica fibers and Rayleigh limit silica fibers at two wavelengths and several oblique angles of incidence.

## References


[1]Twersky, V., "Coherent Scalar Field in Pair-Correlated Random Distributions of Aligned Scatterers," *Journal of Mathematical Physics*, Vol. 18, No. 12, 1977, pp. 2468–2486.

[2]Ishimaru, A., *Wave Propagation and Scattering in Random Media*, Vols. 1 and 2, Academic, New York, 1978.

[3]Lee, S. C., "Dependent Scattering by Parallel Fiber: Effects of Multiple Scattering and Wave Interference," *Journal of Thermophysics and Heat Transfer*, Vol. 6, No. 4, 1992, pp. 589–595.

[4]Twersky, V., "Multiple Scattering of Radiation by an Arbitrary Configuration of Parallel Cylinders," *Journal of the Optical Society of America*, Vol. 24, No. 1, 1952, pp. 42–46.

[5]Twersky, V., "Multiple Scattering of Radiation by an Arbitrary Planar Configuration of Parallel Cylinders and by Two Parallel Cylinders," *Journal of Applied Physics*, Vol. 23, No. 4, 1952, pp. 407–414.

[6]Oloafe, G. O., "Scattering by an Arbitrary Configuration of Parallel Circular Cylinders," *Journal of the Optical Society of America*, Vol. 60, No. 9, 1970, pp. 1233–1236.

[7]Lee, S. C., "Dependent Scattering of an Obliquely Incident Plane Wave by a Collection of Parallel Cylinders," *Journal of Applied Physics*, Vol. 68, No. 10, 1990, pp. 4952–4957.

[8]Lee, S. C., "Scattering by Closely-Spaced Radially-Stratified Parallel Cylinders," *Journal of Quantitative Spectroscopy & Radiative Transfer*, Vol. 48, No. 2, 1992, pp. 119–130.

[9]Lax, M., "Multiple Scattering of Waves. II. The Effective Field in Dense Systems," *Physical Review*, Vol. 85, No. 4, 1952, pp. 621–629.

[10]Bose, S. K., and Mal, A. K., "Longitudinal Shear Waves in a Fiber-Reinforced Composite," *International Journal of Solids and Structures*, Vol. 9, No. 9, 1973, pp. 1075–1085.

[11]Twersky, V., "Propagation in Pair-Correlated Distributions of Small-Spaced Lossy Scatterers," *Journal of the Optical Society of America*, Vol. 69, No. 11, 1979, pp. 1567–1572.

[12]Varadan, V. K., Varadan, V. V., and Pao, Y.-H., "Multiple Scattering of Elastic Waves by Cylinders of Arbitrary Cross Section. I. SH Waves," *Journal of the Acoustical Society of America*, Vol. 63, No. 5, 1978, pp. 1310–1319.

[13]Varadan, V. K., Ma, Y., and Varadan, V. V., "Multiple Scattering of Compressional and Shear Waves by Fiber-Reinforced Composite Materials," *Journal of the Acoustical Society of America*, Vol. 80, No. 1, 1986, pp. 333–339.

[14]Lee, S. C., "Effective Propagation Constants of Fibrous Media Containing Parallel Fibers in the Dependent Scattering Regime," *Journal of Heat Transfer*, Vol. 114, No. 2, 1992, pp. 473–478.

[15]Lee, S. C., "Propagation of Radiation in High-Density Fibrous Composites Containing Coated Fibers," *Journal of Thermophysics and Heat Transfer*, Vol. 7, No. 4, 1993, pp. 637–643.

[16]Kerker, M., *The Scattering of Light and Other Electromagnetic Radiation*, Academic, New York, 1969, Chap. 6.

[17]Barabas, M., "Scattering of a Plane Wave by a Radially-Stratified Tilted Cylinder," *Journal of the Optical Society of America*, Vol. 4, No. 12, 1987, pp. 2240–2248.

[18]Twersky, V., "Transparency of Pair-Correlated Random Distributions of Small Scatterers with Application to Cornea," *Journal of the Optical Society of America*, Vol. 65, No. 2, 1975, pp. 524–530.

[19]Wood, W. W., "NpT-Ensemble Monte Carlo Calculations for the Hard Disk Fluid," *Journal of Chemical Physics*, Vol. 52, No. 2, 1970, pp. 729–741.